

# Boundary-mediated electron-electron interactions in quantum point contacts

V. T. Renard<sup>1,2</sup>, O. A. Tkachenko<sup>2,3</sup>, V. A. Tkachenko<sup>3</sup>, T. Ota<sup>1</sup>, N. Kumada<sup>1</sup>, J-C Portal<sup>2,4</sup>, Y. Hirayama<sup>1,5,6</sup>.

<sup>1</sup> NTT Basic Research Laboratories, NTT Corporation 3-1 Morinosato Wakamiya, Atsugi 243-0198, Japan

<sup>2</sup> GHMFL-CNRS, BP 166, F-38042, Grenoble Cedex 9, France,

<sup>3</sup> Institute of Semiconductor Physics, 630090 Novosibirsk, Russia,

<sup>4</sup> INSA and Institut Universitaire de France, F-31077, Toulouse Cedex 4, France.

<sup>5</sup> SORST-JST 4-1-8 Honmachi, Kawaguchi, Saitama 331-0012, Japan and

<sup>6</sup> Department of Physics, Tohoku University, Sendai 980-8578, Japan

(Dated: March 28, 2008)

An unusual increase of the conductance with temperature is observed in clean quantum point contacts for conductances larger than  $2e^2/h$ . At the same time a positive magnetoresistance arises at high temperatures. A model accounting for electron-electron interactions mediated by boundaries (scattering on Friedel oscillations) qualitatively describes the observation. It is supported by numerical simulation at zero magnetic field.

Quantum point contacts (QPC) are usually formed when two wide 2D conducting regions are connected by a small constriction. They exhibit a number of intriguing phenomena among which conductance quantization [1, 2] is the most emblematic. Nowadays QPCs are very common tools for condensed matter physicists. Examples of recent applications include nuclear spin manipulation, solid state electron optics or precise electron counting [3]. Recently, the puzzling low conductance “0.7 anomaly” [4] has attracted most of the attention since it is related to electron-electron (e-e) interactions. But apart “0.7 anomaly” it is commonly believed that the physics of QPCs is well understood using a single-particle picture (See Ref.5 and references therein). On the contrary, it is well known that the properties of two-dimensional electron gases (2DEGs) dramatically depend on interactions [6, 7, 8, 9, 10]. The related corrections to the conductance and tunnelling density of states have their origin in Friedel oscillations (FO) of electron density around impurities. Friedel oscillations are also known to appear at boundaries [11, 12, 13] and could therefore affect the properties of nano-scale devices. Interestingly, boundary mediated FOs were recently shown to be possibly involved in “0.7 anomaly” physics [14] but this subject is still highly debated [15].

In this context we show that e-e interactions can have a significant influence on transport properties of clean quantum point contacts even in the large conductance regime ( $G \gg 2e^2/h$ ). We used a combination of relatively low electron densities, high mobility and low series resistance to clearly uncover the effects of e-e interactions. It increases interactions due to reduced screening and ensures that impurity scattering can be disregarded. Starting from the second conductance step, the average slope of the conductance versus gate voltage linearly increases with increasing temperature  $T$ . At the same time, the low field magneto-resistance (MR) is non-monotonic at high  $T$  and strongly temperature dependent. Some of our findings are present, although not as evident, in previous works [16, 17, 18, 19]. They are consistent with

a model of e-e interaction mediated by boundaries which is supported by numerical simulation at  $B = 0$  T.

The quantum point contacts were defined employing a split-gates lateral depletion technique [20] on high mobility GaAs quantum wells [21]. Needle and square shaped samples of various sizes were used to check the influence of the geometry (see Table I). All samples have back gate to tune the electron density and some samples have a  $0.2 \mu\text{m}$ -wide center gate to obtain better defined conductance quantization steps when grounded [22]. Four-terminal resistance measurements were carried out between 350 mK and 10 K with a standard low-frequency technique at small excitation voltage  $< 20 \mu\text{V}$  to avoid heating effects. Any obvious temperature dependence (activated parallel conduction, anomalous temperature dependence of the series 2DEG or leakage of the gates) was excluded [23]. More than ten samples showed a qualitatively similar behavior.

TABLE I: Summary of the samples (for the wafer and Hall bar see [21]).

Sample	Wafer	Hall bar	point contact	center gate
Square1	1	1	W=0.6 $\mu\text{m}$ ; L=0.4 $\mu\text{m}$	yes
Square2	1	1	W=0.6 $\mu\text{m}$ ; L=1 $\mu\text{m}$	yes
Needle1	2	2	W=0.8 $\mu\text{m}$	no
Needle2	2	2	W=0.6 $\mu\text{m}$	no

Figure 1a shows the conductance  $G$  of the sample Square1 as the split-gate voltage  $V_{sp}$  is varied for different temperatures. The small ( $\sim 15\Omega$ ) 2DEG series resistance was not subtracted. At low  $T$  the conductance is quantized to exact integer values of  $2 \times e^2/h$ . Note that the “0.7 anomaly” is observed. Increasing temperature not only shrinks the plateaus but also increases the overall slope of  $G(V_{sp})$  resulting in the increase of conductance with  $T$ . Such a change in the slope of the conductance is not expected from a simple energy averaging, which produces fix temperature independent points

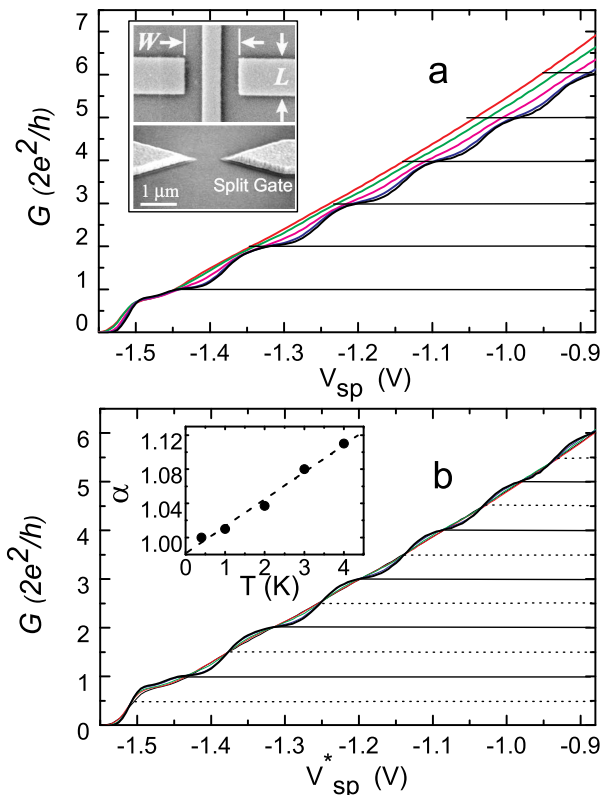


FIG. 1: a) Conductance of the sample Square1 as a function of  $V_{sp}$  (From top to bottom  $T=4$  K, 3 K, 2 K, 1 K and 350 mK). The inset shows SEM images illustrating possible shapes of the point contacts. b) Conductance as a function of the scaled split-gate voltage  $V_{sp}^*$  for the same temperatures. The inset shows the scaling parameter  $\alpha$ .

in the conductance located at integers of  $e^2/h$  [24]. Regions with alternatively positive or negative temperature dependence should be separated by these fixed points. This is not observed in our experiment. It is however possible to restore this behavior by a phenomenological approach. For each temperature a new effective split-gate voltage can be calculated  $V_{sp}^* = V_p + \alpha(T) \times (V_{sp} - V_p)$  to superpose the curve to the low temperature one (See Fig. 1b). Here,  $V_p$  is the pinch off voltage and  $\alpha$  is the scaling parameter. The strong linear temperature dependence of  $\alpha$  points at quantum effects, possibly e-e interactions.

In the Hartree-Fock approximation scattering on the potential created by all the other electrons can be considered as the origin of e-e interactions effects [6, 7, 8, 9, 12, 13]. This potential is connected to the formation of Friedel oscillations of the electron density close to scatterers (defects or boundaries) due to interferences between incoming and reflected electron waves. Spatial variations of their density results in a varying effective potential seen by conducting electrons. In our case the QPC is clean and FOs are created at the boundaries of the constriction. They affect its conductance in two different ways. At low  $T$  when the thermal length  $l_T$  exceeds  $W$

the QPC width, FOs located in the 2DEG can reduce the conductance at a plateau via scattering of emitted electrons back to the QPC [11]. As  $T$  is increased these oscillations are damped and conductance plateaus reach ideal integer value of  $2 \times e^2/h$  [25]. When  $l_T \approx W$  there remain only FOs located inside the QPC. This corresponds to our experimental conditions ( $l_T \approx 1 \mu\text{m}$  at  $T = 300$  mK). As  $T$  is further increased the transverse oscillations inside the QPC are damped thus effectively widening the constriction (or equivalently shifting 1D energy levels). One has to compensate by applying a lower  $V_{sp}$  to obtain a comparable value of conductance (the curves shift to the left). The scaling can be qualitatively understood as follows. Electrostatically defined QPCs have a parabolic cross section  $U = m^* \omega^2 x^2 / 2$ ,  $m^*$  is the effective mass. The width of the channel can be defined as  $W = (2/\omega) \sqrt{2E_F/m^*}$ , where  $E_F$  is the Fermi level in 2DEG reservoirs. One-dimensional energy levels are written  $E_n = (n + 1/2)\hbar\omega$  and in a constant capacitance model  $W$  is proportional to  $V_{sp} - V_p$ . It follows that  $\Delta E_n/E_n \propto \Delta\omega/\omega \propto \Delta W/W \propto \Delta(V_{sp} - V_p)/(V_{sp} - V_p)$ . In analogy to the 2D case where the conductivity  $\sigma$  is renormalized as  $\Delta\sigma/\sigma \sim \beta \times T/E_F$  in the ballistic regime of interaction [8] we expect that  $\Delta E_n/E_n \sim \beta \times T/E_F$  when  $E_n \sim E_F$  (the interaction-induced shift  $\Delta E_n$  of the closest to Fermi level subband only is considered). Here,  $\beta$  is the interaction parameter. This leads to the rescaling  $V_{sp} \rightarrow V_{sp}^* = V_p + \alpha(T)(V_{sp} - V_p)$  with  $\alpha(T) \propto T$  as measured.

This result is consistent with a numerical non-self-consistent Hartree-Fock simulation. The principle of the computation is first to calculate the local electron density  $n(x, y, T, \mu)$  solving the one-particle Schrödinger equation in a “soft wall” electrostatic potential for different chemical potential  $\mu$  and temperature  $T$ . Indeed, instead of calculating the conductance as a function of  $V_{sp}$  for a varying potential  $U_0(x, y, V_{sp})$  and fixed  $\mu$ , we chose to fix the electrostatic potential and vary the chemical potential. This greatly simplifies the calculation because the wave-functions are calculated only once. It is valid for small interval of split gate voltage (between two conductance steps). Numerical technique and parameters are described in Ref. 26, 27. In analogy to the 2D case, the interaction correction to the potential is computed as follows  $\delta U(x, y, T, \mu) = \beta \delta n(x, y, T, T^*, \mu)/D$ , where  $\beta$  is the interaction parameter,  $D$  is the 2D density of states,  $\delta n(x, y, T, \mu) = n(x, y, T, \mu) - n(x, y, T^*, \mu)$  and  $T^*$  a temperature high enough to suppress FOs. The obtained correction which includes only  $T$ -dependent terms is then used to solve the transmission problem in the total potential which is now a function of  $T$  and  $\mu$  [26]. Contrary to 2D systems containing impurities [8, 9] it is not possible to relate the interaction parameter  $\beta$  to the interaction constant  $F_0$  in a simple way. Close to the boundaries the electron density drops to zero. This drop is not completely abrupt and the first Friedel oscillation

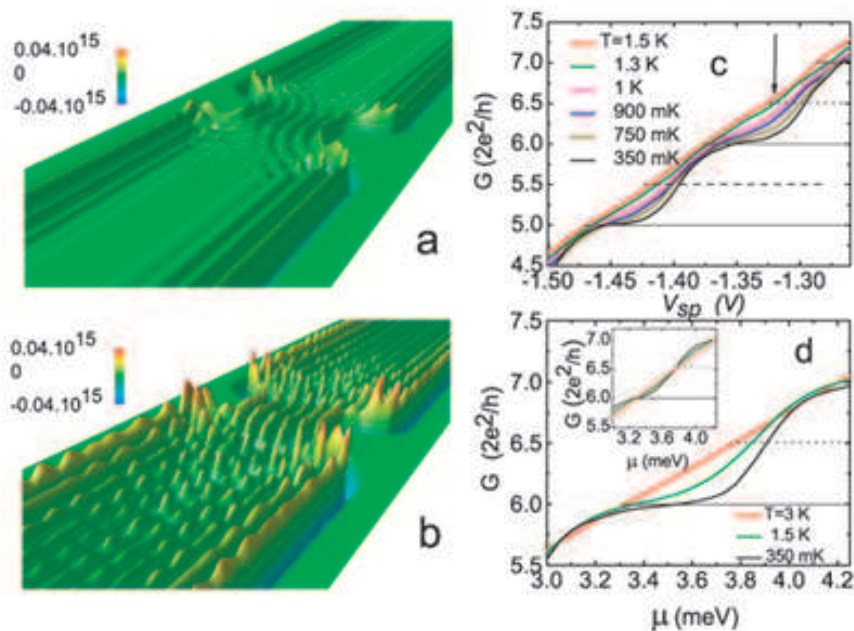


FIG. 2: Calculated correction to the electron density due to Friedel oscillations at  $G \approx 6 \times 2e^2/h$  for  $T=3.5$  K (a) and  $T=350$  mK (b). The scale is  $m^{-2}$ . This clearly illustrates the rise of the interaction potential as  $T$  decreases. c) Conductance of the sample Needle1 for different temperature. The vertical arrow corresponds to the voltage at which Fig. 3a was recorded. d) Calculated conductance at a similar value of conductance. The inset shows the calculated conductance neglecting e-e interactions.

develops in rarefied weakly-screening electron gas where e-e interactions become particularly strong. This is taken into account in our simulation by the large value of the parameter  $\beta = -6$ . Figures 2a and b show the obtained correction to the electrons density  $\delta n(x, y)$  in the vicinity of the constriction at  $G \approx 6 \times e^2/h$  for  $T=3.5$  K (a) and  $T=350$  mK (b). This clearly illustrates the formation of FOs as  $T$  is decreased. Note that pronounced features are demonstrated despite the use of a “soft wall” model. Figures 2c and d compare the experimental conductance of the sample Needle1 to the conductance calculated by the method described above. In both cases the fix temperature independent points are missing and the conductance is on average increasing with temperature. A test of the model consists in neglecting the interaction term of the scattering potential (i.e. setting the interaction parameter  $\beta$  to 0) which restores the dependence for energy averaging as expected (Inset to Fig. 2d). An overall good qualitative agreement is obtained between computer and real experiments which further confirms the qualitative understanding.

In general, the magnetoresistance reveals important informations about scattering, coherent processes and e-e interactions [9]. Figure 3a shows that beside the unusual temperature dependence at  $B = 0$  T the samples present an unexpected field dependence. The data displayed were measured for sample Needle1 at  $G \approx 6 \times 2e^2/h$  (see arrow in Fig. 2c). At high temperature, the magnetoresistance presents a maximum around  $B = 10$  mT and becomes negative at higher fields. At low  $T$  the resistance decreases with  $B$  at all magnetic fields. The high field slope of the MR is  $T$ -dependent. Note that the maximum moves to lower fields in QPCs with larger width (not shown).

A linear negative MR with a slope inversely proportional to the width of the channel is known to appear in QPCs [28]. The increased slope at low temperature that we observe is consistent with the observation at  $B = 0$  T which lead to the conclusion that e-e interactions could in principle reduce the effective width of the channel at low  $T$ . As for the positive MR, it cannot be attributed to diffuse boundary scattering which has very different characteristics [29]. In particular it is  $T$ -independent and absent in short constrictions. Similarly, the interplay of boundary scattering and electron collisions [30] can be discarded. Finally, commensurability of electron trajectories with the voltage probes can be ruled out since very different Hall bar geometries were tested (Table. I).

The absence of positive MR at low  $T$  confirms that the observed quantum effect is due to e-e interaction and is not an interference effect (i.e. Weak anti-localization) which should increase at low  $T$ . Similarly to 2D systems [31], it can most likely be explained by a variation of the parameter  $\beta$  at small magnetic fields which is only visible at high  $T$ . Note that simulations with  $B$ -independent  $\beta$  did not produce the positive MR. Figure 3b and c demonstrates that the magneto-resistance depends on the electron density and detailed geometry of the point contacts. Carefully adjusting the back- and split-gate voltages, the conductance  $G(T = 4K, B = 0T)$  of the sample Needle2 was tuned to the same value ( $\approx 13 \times 2e^2/h$ ) for two different electron densities. Although qualitatively similar, the effect is found to be more pronounced at the lower density. This is consistent with the Friedel oscillation picture which should have in principle smaller effect at high densities when the system resembles a non-interacting Fermi liquid. Figure 3c compares the results of the sample Needle2 to the effect obtained in the sample Square2

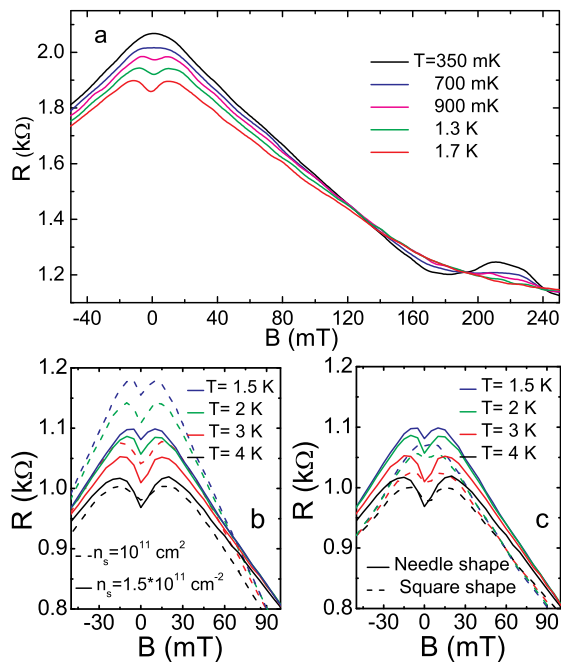


FIG. 3: a) Resistance of the sample Needle1 at the gate voltage indicated by an arrow in Fig. 2c. b) Resistance of the sample Needle2 for the electron density  $n_s = 1 \times 10^{11} \text{ cm}^{-2}$  (dash) and  $n_s = 1.5 \times 10^{11} \text{ cm}^{-2}$  (solid) for  $G(T = 4\text{K}) \approx 13 \times 2e^2/h$ . c) Resistance of Needle2 (solid) and Square2 (dot) for  $n_s = 1.5 \times 10^{11} \text{ cm}^{-2}$  and  $G(T = 4\text{K}) \approx 13 \times 2e^2/h$ .

at the same density and conductance. The temperature dependence at  $B = 0 \text{ T}$  is comparable but the field dependence is much more pronounced for the sample Needle2 which has smoother entrances. The geometry dependence therefore appears to be a very interesting tool to study the effect of magnetic field on the measured effect. The positive MR raises interesting questions about the influence of low magnetic field on Friedel oscillations and requires additional theoretical work.

We believe that the presented deviations have not been observed in regular point contacts (for example in Ref. [24]) due to the lower mobility and higher density in these experiments. Indeed, Friedel oscillations are known to depend exponentially on disorder and interaction. However, recent measurements on similar samples show similar phenomenology (see Ref. 16, 17, 18 for the conductance quantization and Ref. 19 for the MR) indicating that our observation is a general effect. It could have particular importance in nano-scale electronics since boundaries dominate transport properties in nano-devices (electrostatically defined quantum dots, rings, Y-junctions etc.).

We are very grateful to I. Gornyi, A. Dmitriev, K. Takashina, Y. Tokura, K. Pyshkin for helpful discussions and K. Muraki for providing some samples. O.A.T. acknowledges UJF for the invitation as “Maître de Conférences”, the Supercomputing Siberian center and

CNRS/IDRIS (project 61778). Part of this work was supported by CNRS/RAS agreement between ISP Novosibirsk and GHMFL Grenoble.

- 
- [1] B. J. Van Wees *et al. Phys. Rev. Lett.* **60**, 848 (1988).
  - [2] D. A. Wharam *et al. J. Phys. C.* **21**, L209 (1988).
  - [3] G. Yusa *et al. Nature* **434**, 1001 (2005); B. J. Le Roy *et al. Phys. Rev. Lett.* **94**, 126801 (2005); T. Fujisawa *et al. Science.* **312**, 1634 (2006).
  - [4] K. J. Thomas *et al. Phys. Rev. Lett.* **77**, 135 (1996).
  - [5] C. W. J. Beenakker & H. Van Houten *Solid State Physics.* **44**, 1 (1991).
  - [6] B. L. Altshuler & A. G. Aronov Electron-electron interaction in disordered systems. (A. L. Efros, M. Pollak, Amsterdam, 1985).
  - [7] A. Rudin, I. Aleiner & L. Glazman *Phys. Rev. B* **55**, 9322 (1997).
  - [8] G. Zala, B. N. Narozhny, & I. Aleiner *Phys. Rev. B* **64**, 214204 (2001).
  - [9] I. V. Gornyi & A. D. Mirlin *Phys. Rev. Lett.* **90**, 076801 (2003); *Phys. Rev. B* **69**, 045313 (2004).
  - [10] V. T. Renard *et al. Phys. Rev. B* **72**, 075313 (2005).
  - [11] A. Alekseev & V. Cheianov *Phys. Rev. B* **57**, 6834 (1998).
  - [12] I. Aleiner & L. Glazman *Phys. Rev. B* **57**, 9608 (1998).
  - [13] V. A. Sablikov *JETP Lett.* **84**, 404 (2006); B. S. Shchamkhalova & V. A. Sablikov *J. Phys.: Condens. Matter*, v. 19, 156221 (2007).
  - [14] T. Rejec & Y. Meir *Nature* **442**, 900 (2006).
  - [15] S. Ihnatsenka & I. Zozoulenko *Phys. Rev. B* **76**, 045338 (2007).
  - [16] A. E. Hansen, A. Kristensen, H. Bruus, *Proceedings of NANO-7/ECOSS-21. Malmö, Sweden. 24-28 June 2002.*
  - [17] K. Pyshkin (Phd Thesis, University of Cambridge, 2000).
  - [18] S. Cronenwett *et al. Phys. Rev. Lett.* **88**, 226805 (2002).
  - [19] Y. Feng *et al. J. Vac. Sci. Technol. A* **18**, 730 (1999).
  - [20] T. J. Thornton *et al. Phys. Rev. Lett.* **56**, 1198 (1986).
  - [21] Two wafers were used with the mobility  $\mu_1 \approx 4 \times 10^6 \text{ cm}^2/\text{Vs}$  and  $\mu_2 \approx 3 \times 10^6 \text{ cm}^2/\text{Vs}$  for a density  $n_{s1} = 1.5 \times 10^{11}$  and  $n_{s2} = 1 \times 10^{11}$ . They were processed into  $10 \mu\text{m}$  wide (type 1) and  $100 \mu\text{m}$  wide (type 2) Hall bars.
  - [22] H. M. Lee, K. Muraki, E. Y. Chang, & Y. Hirayama, *J. App. Phys.* **100**, 043701 (2006).
  - [23] Hall measurements show that the electron density is  $T$ -independent. The resistance of the 2DEG decreases only by a few Ohms between high and low  $T$  which makes this source of  $T$ -dependence incompatible with the observation. Also, the split gate’s leakage current was monitored to be smaller than  $20 \text{ pA}$  at all voltages and  $T$ .
  - [24] B. J. Van Wees *et al. Phys. Rev. B* **43**, 12431 (1991).
  - [25] A. Yacoby *et al. Phys. Rev. Lett.* **77**, 4612 (1996)
  - [26] The computation region was  $3 \mu\text{m}$  long and  $0.7 \mu\text{m}$  wide. The constriction is  $250 \text{ nm}$  wide in the model. The calculation step along  $x$  and  $y$  was  $5 \text{ nm}$ , the energy step was  $10^{-3} \text{ meV}$ . Usual hopping constant for GaAs were used.
  - [27] T. Usuki *et al. Phys. Rev. B* **52**, 8244 (1995).
  - [28] H. Van Houten *et al. Phys. Rev. B* **37**, 8534 (1988).
  - [29] T. J. Thornton *et al. Phys. Rev. Lett.* **63**, 2128 (1989); F. Rahman *et al. Semicond. Sci. Technol.* **14**, 478 (1999).
  - [30] R. N. Gurzhi, A. N. Kalinenko, & A. I. Kopeliovich *Phys. Rev. Lett.* **74**, 3872 (1995).

- [31] G. Zala, B. N. Narozhny, & I. Aleiner *Phys. Rev. B* **65**, 020201 (2001).